Calmodulin Activation of the Ca^{2+} Pump Revealed by Fluorescent Chelator Dyes in Human Red Blood Cell Ghosts

MARILYN R. JAMES-KRACKE

From the Department of Pharmacology, University of Missouri-Columbia, Columbia, Missouri 65212

ABSTRACT Ca^{2+} transport in red blood cell ghosts was monitored with fura2 or quin2 incorporated as the free acid during resealing. This is the first report of active transport monitored by the fluorescent intensity of the chelator dyes fura2 (5–50 μM) or quin2 (250 μM) in hemoglobin-depleted ghosts. Since there are no intracellular compartments in ghosts and the intracellular concentrations of all assay chelator substances including calmodulin (CaM), the dyes, and ATP could be set, the intracellular concentrations of free and total Ca ($[Ca_{free}]_i$ and $[Ca_{total}]_i$) could be calculated during the transport. Ghosts prepared with or without CaM rapidly extruded Ca^{2+} to a steady-state concentration of 60–100 nM. A 10^4-fold gradient for Ca^{2+} was routinely produced in medium containing 1 mM Ca^{2+}. During active Ca^{2+} extrusion, $d[Ca_{free}]_i/dt$ was a second order function of $[Ca_{free}]_i$ and was independent of the dye concentration, whereas $d[Ca_{total}]_i/dt$ increased as a first order function of both the $[Ca_{free}]_i$ and the concentration of the Ca:dye complex. CaM (5 μM) increased $d[Ca_{total}]_i/dt$ by 400% at 1 μM $[Ca_{free}]_i$, while $d[Ca_{free}]_i/dt$ increased by only 25%. From a series of experiments we conclude that chelated forms of Ca^{2+} serve as substrates for the pump under permissive control of the $[Ca_{free}]_i$, and this dual effect may explain cooperativity. Free Ca^{2+} is extruded, and probably also Ca^{2+} bound to CaM or other chelators, while CaM and the chelators are retained in the cell.

INTRODUCTION

The properties of the Ca^{2+} ATPase and pump have been characterized most extensively in a variety of preparations from red cells including intact cells, resealed ghosts, membrane fragments, and vesicles. Until the Ca^{2+}-sensitive fluorescent dyes (quin2, bapta, benz2, and fura2) were introduced (Tsien et al., 1982; Grynkiewicz et al., 1985), a method was not available to study active Ca^{2+} transport over the nanomolar range of intracellular free calcium concentrations ($[Ca_{free}]_i$) in intact red cells or ghosts (Schatzmann, 1975). These dyes can be introduced into intact red cells by using the permeant ester forms (Lew et al., 1982*b*; Tiffert et al., 1984; Murphy et al., 1986; David-Dufilho et al., 1988) or can be incorporated directly into ghosts as

Address reprint requests to Dr. Marilyn R. James-Kracke, Department of Pharmacology, University of Missouri, School of Medicine, M517B Medical Sciences Bldg., Columbia, MO 65212.

J. GEN. PHYSIOL. © The Rockefeller University Press · 0022-1295/92/01/0041/22 $2.00
Volume 99 January 1992 41–62

the free acid impermeant form during resealing (James-Kracke and Chai, 1986; James-Kracke and Freedman, 1986). The latter approach avoids several problems that occur when using the ester forms of the dyes in intact cells (Tsien et al., 1982; Tiffert et al., 1984; Highsmith et al., 1986; Scanlon et al., 1987; David-Dufilho et al., 1988)[1] and more importantly affords several advantages for Ca^{2+} transport studies. In ghosts, the quenching by hemoglobin (Lew et al., 1982*b*) can be eliminated and the intracellular ATP, Ca^{2+}, Mg^{2+}, calmodulin (CaM), and dye concentrations ([D]) can be controlled during the loading, which is not possible in intact red cells. Additionally, transport is monitored only in tightly resealed ghosts because leaky and prematurely resealed ghosts do not retain the dye. Furthermore, $[Ca_{free}]_i$ is calculated directly from the fluorescence and is independent of the volume and protein contents of these latter types of ghosts. In addition to $[Ca_{free}]_i$, the total intracellular calcium concentration ($[Ca_{total}]_i$) can be accurately calculated on a faster time scale (every second) than is possible by ^{45}Ca (Lew et al., 1982*b*) or NMR (Murphy et al., 1986) approaches.

At rest $[Ca_{free}]_i$ is reported to be as low as 26–78 nM in erythrocytes (Lew et al., 1982*b*; Murphy et al., 1986; David-Dufilho et al., 1988). These levels are below the 100–200-nM threshold Ca^{2+} concentration required by CaM to stimulate Ca^{2+}-ATPase activity (Bond and Clough, 1973; Farrance and Vincenzi, 1977; Foder and Scharff, 1981; Muallem and Karlish, 1982; Scharff and Foder, 1982; Garrahan, 1986; Villalobo et al., 1986). The main purpose of this study was to determine how CaM activates the Ca^{2+} pump over the physiological range of $[Ca_{free}]_i$.

This is the first full report of Ca^{2+} transport over the nanomolar range in red cell ghosts. Ghosts were loaded with fura2 or quin2, Ca, an ATP-regenerating system, and CaM at various concentrations. A combination of techniques (Schatzmann, 1973; Larsen et al., 1978; Muallem and Karlish, 1979; Kratje et al., 1983) increased the rate of resealing, conserved ATP, and prevented premature Ca^{2+} extrusion for improved transport studies. An interesting effect of the dyes on the Ca^{2+} pump activity was noted and may be related to the paradoxical "EGTA effect" (Al-jobore and Roufogalis, 1981; Kotogal et al., 1983; Rega, 1986*b*; Carafoli, 1991) or the proposal that the pump may be activated by any negatively charged molecule with a hydrophobic moiety (Niggli et al., 1981).

MATERIALS AND METHODS

Preparation of Ghosts and Loading with Fura2 or Quin2 during Resealing

Fura2 was not loaded as the permeant ester as in most other studies. Precise concentrations of the free acid form of the dye were incorporated during the preparation of ghosts when the cells were opened. Fresh human blood was heparinized and the red cells were washed four times by centrifugation in a buffer containing 145 mM NaCl, 5 mM KCl, and 5 mM HEPES, pH 7.4, at 4°C. Ghost membranes were prepared under divalent ion–free conditions to remove CaM and

[1] $[Ca_{free}]_i$ measurements in intact red cells loaded with 1 μM fura2/am were less satisfactory. It took >2 h to produce sufficient fluorescence to be detected in the intensely pigmented cells and the deesterification was never complete. Dye continued to escape from cells as permeant intermediates of fura2/am (David-Dufilho et al., 1988) or because cells gradually lyse as ATP is depleted during formaldehyde production (Tiffert et al., 1984). Also the CaM concentration could not be controlled in intact cells. Therefore ghosts were more suitable for these studies.

hemoglobin from the membranes[2] (Roufogalis, 1979; Al-jobore and Roufogalis, 1981; Foder and Scharff, 1981). Packed red cells (1 ml) were lysed while stirring on ice for 10 min in 100 ml of hypotonic lysing solution containing 15 mM KCl, 0.01 mM EDTA, 1 mM EGTA, and 5 mM HEPES, pH 6.0, to reduce premature spontaneous resealing (Richards and Eisner, 1982). The membranes were centrifuged at 12,000 *g* for 10 min and washed in 100 ml of lysing solution without EGTA, and again in 100 ml of EGTA-free lysing solution containing 2 mM Mg^{2+}. Membrane pellets were concentrated in 4 ml of this last solution. This three-wash method diluted most cytosolic components 4 million-fold.

To load each milliliter of ghosts, 0.85 ml of concentrated membrane suspension and 5–50 μM fura2 or 250 μM quin2 were added, plus 0.25–1 mM $CaCl_2$. The initial $[Ca_{total}]_i$ in the ghost is lower than this because the ghosts extrude a considerable amount of Ca during the resealing process. To prepare "active" ghosts for efflux experiments, 2 mM ATP and an ATP-regenerating system of 5 mM phosphocreatine and 8–32 μg/ml (1–4 u/ml) phosphocreatine kinase (Glynn and Hoffman, 1971) as well as 0–5 μM CaM were added. Na orthovanadate (50 μM) (Cantley et al., 1978; Rossi et al., 1981) was added to inhibit premature extrusion of Ca^{2+} and to conserve ATP. The vanadate inhibits but does not completely stop the efflux. Therefore, it is still necessary to reseal rapidly as described below.

The osmolarity was corrected by adding 41.7 μl of 3 M KCl (140 mM final KCl). The pH was adjusted to 7.4 by adding 20 μl of 250 mM HEPES, pH 7.6 (10 mM final HEPES). The ghosts were warmed to 37°C rapidly for 30 s and then chilled. Ghosts were resealed originally by incubating in a 37°C water bath for 6 min in plastic centrifuge tubes and then chilled. Then corex tubes, which transfer heat faster, were used in a hot block at 60°C while monitoring temperature to 37°C with a thermistor. Although resealing can occur in ~10 s (Kratje et al., 1983) (which conserves ATP without using vanadate), resealing was less complete. A "hot-reseal with vanadate" method over 40 s (10 s in a 60°C bath and 30 s in a 37°C bath) prevented premature extrusion and yielded the fastest transport rates to the lowest steady-state levels of $[Ca_{free}]_i$.

The resealed ghosts were centrifuged at 12,000 *g* at 4°C for 10 min and washed with 10 ml of a buffer containing 145 mM NaCl, 5 mM KCl, 1 mM $CaCl_2$, 2 mM $MgCl_2$, and 5 mM HEPES, pH 7.4. The washes were repeated four times to remove vanadate[3] and all the unincorporated quin2 and fura2. Washed resealed ghosts were resuspended in 1 ml of the same ice-cold buffer (~10% hematocrit).

For influx experiments in active ghosts, ghosts were resealed without Ca^{2+} (or vanadate) and washed with Ca-free buffer containing 100 μM EGTA. For influx studies in "passive" ghosts, the ATP-regenerating system, Ca^{2+}, vanadate, and CaM were omitted. Resealing of ghosts was equally effective with or without Ca^{2+}, since they retained equivalent amounts of dye. The "autofluorescence" of ghosts without dye at 340 and 380 nm was subtracted (<1%) before calculation of $[Ca_{free}]_i$.

[2] Removal of CaM from the membranes was confirmed by electrophoresis on a 12% SDS acrylamide gel. No protein bands from 16,700 to 20,000 D over the molecular weight range reported for calmodulin (Klee et al., 1980) were observed. Membranes prepared without the initial EGTA treatment in the first wash had a faint band at 20,100 D.

[3] Vanadate escapes through DIDS-sensitive anion exchangers, which are numerous in the red cell membrane (Cantley et al., 1978; Varecka and Carafoli, 1982). This was directly measured by Cantley et al. (1978) using ^{48}V. In our experiments, the washout of vanadate was indirectly measured. Ghosts exposed to 200 μM vanadate for 10 min in the medium did not pump, but after they were washed twice in ice-cold medium in a refrigerated microfuge and reintroduced into warm medium, they extruded Ca^{2+} rapidly to the usual low $[Ca_{free}]_i$. The escape of vanadate was blocked in ghosts prepared from red cells pretreated with 10 μM DIDS for 1 h at 37°C.

Fluorescence Measurements and Calculation of $[Ca_{free}]_i$

Fluorescence was measured in a computerized spectrofluorometer (model MPF-66; Perkin-Elmer Corp., Norwalk, CT) (5-nm slits; quin2 excitation 339 nm, emission 492 nm; fura2 excitation 340 nm [and 380 nm, ratio method], emission 502 nm). The sample compartment was temperature controlled to 37°C and magnetically stirred. To start the transport assay, ice-cold ghosts (250 μl) were diluted 10-fold in buffer at 37°C in the cuvette (final hematocrit ~1%). Fluorescence time courses were converted to $[Ca_{free}]_i$ every second for the single excitation method (Tsien et al., 1982) or every 9.5 s by the 340/380 nm excitation ratio method (Grynkiewicz et al., 1985). More recent experiments on the Spex (Edison, NJ) CM1T111 fluorometer with a ratio time of 1 s have yielded rates of extrusion equal to those measured on the MPF-66.

$[Ca_{free}]_i = K_d \times (F - F_{min})/(F_{max} - F)$ by the single excitation method (Tsien et al., 1982; Grynkiewicz et al., 1985) or $[Ca_{free}]_i = K_d \times (Sf380/b380) \times (R - R_{min})/(R_{max} - R)$ by the ratio method (Grynkiewicz et al., 1985). F_{max} and R_{max} were determined in saturating Ca^{2+} (1 mM) after adding 2 μM ionomycin or 0.02% Triton X-100. F_{min} and R_{min} were determined when Ca^{2+} was reduced below 1 nM by adding 4 mM EGTA and 50 mM Tris base (final pH > 8.3; Tsien et al., 1982). The constants for the Ca-bound maximum ratio (R_{max}), Ca-free minimum ratio (R_{min}), and the ratio of the intensities of the free and bound dye forms at 380 nm (Sf380/b380) were 27 ± 0.82, 0.84 ± 0.01, and 8.03 ± 0.38, respectively (n = 8, 4 in calibration solutions and 4 in ghosts; i.e., these constants were the same in ghosts and calibration solutions from the same dye lot, but they varied somewhat with dye lot (R_{max} ranged from 24 to 31).

The K_d's for quin2 and fura2 binding to Ca^{2+} were determined in calibration solutions with ionic compositions similar to those used to load ghosts at pH 7.4 (Fig. 1) since at pH 7.4 these were expected to be lower than those reported at pH 7.1 (Tsien et al., 1982; Grynkiewicz et al., 1985) as expected (Uto et al., 1991). The K_d for quin2 was 89 nM with 2 mM $MgCl_2$ (46 nM without Mg^{2+}). The K_d for fura2 was 115 nM with 2 mM Mg^{2+} (79 nM without Mg^{2+}) (Fig. 1). Since the free Mg^{2+} would be less than 2 mM in the presence of 2 mM ATP, the calculations, using the higher K_d's (89 and 115 nM), represent the upper limit of $[Ca_{free}]_i$.

Calculation of $[Ca_{total}]_i$

$[Ca_{total}]_i = [Ca_{free}]_i + ([Ca_{free}]_i \times [D_{total}])/(K_d^D + [Ca_{free}]_i) + ([Ca_{free}]_i [4 \times CaM_{total}])/(K_d^{CaM} + [Ca_{free}]_i) + ([Ca_{free}]_i \times [EGTA]_{total})/K_d^{EGTA} + [Ca_{free}]_i)$. For the calculation we assumed that CaM binds 4 Ca^{2+} with equal affinity with an apparent K_d of 1 μM (Klee et al., 1980). In contrast to those ghosts prepared without divalent ion depletion, ghosts prepared from Mg-free EGTA-treated membranes were observed not to shrink by a sensitive light scatter measurement (modified from Knauf et al., 1977). It has been observed that a regulatory protein for control of the Gardos effect is removed by EGTA treatment of red cell vesicles (Lew et al., 1982*a*; Plishker et al., 1986). Therefore, the final total [D] ($[D_{total}]$), ATP, and [CaM] in the ghosts equaled the concentrations during loading. The Ca^{2+} binding to ATP^{-4} at pH 7.4 (K_d 315 μM) in the presence of 2 mM $MgCl_2$ (K_d 11 μM) below 1 μM $[Ca_{free}]_i$ was <2% or 0.2% of the total in fura2- and quin2-loaded ghosts, respectively, and therefore was omitted from the routine calculations.

Calculation of $d[Ca_{free}]_i/dt$ and $d[Ca_{total}]_i/dt$

$d[Ca_{free}]_i/dt$ and $d[Ca_{total}]_i/dt$ were calculated by a least-squares fit program which analyzed the slope of successive series of three points along the curves ($[Ca_{free}]_i$ or $[Ca_{total}]_i$ vs. time) as a function of $[Ca_{free}]_i$ or $[Ca_{total}]_i$ (ordinate midpoint) or the concentration of the Ca:dye complex ([CaD]). Rates from data obtained on the Spex fluorometer were analyzed as a least-squares fit to 24 points at a 1-s ratio time.

Graphics

Figures were drawn by a computer graphics program directly from data files (Fancy Graf, model 7500 computer; Perkin-Elmer Corp.).

Reagents

Quin2 and TPEN were purchased from Calbiochem Corp. (La Jolla, CA). Fura2 was purchased from either Calbiochem Corp. or Molecular Probes, Inc. (Eugene, OR). ATP, CaM (from human blood), phosphocreatine, phosphocreatine kinase (from rabbit brain, type IV), vana-

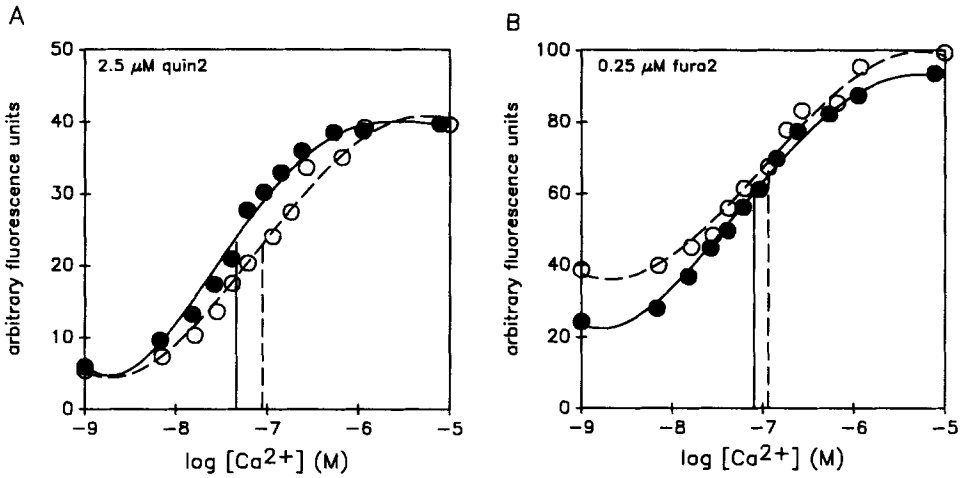

FIGURE 1. Calibration curves for quin2 (*A*) and fura2 (*B*) at pH 7.4. With constants for EGTA ionization (Blinks et al., 1982) the K_d for Ca^{2+} and EGTA at pH 7.4 is 60.2 nM. Ca-EGTA buffers were prepared in 150 mM KCl, 20 mM HEPES, pH 7.4, at 37°C with 1 mM EGTA and 0–1 mM $CaCl_2$ calculated to result in free $[Ca^{2+}]$ from < 1 nM to 7.75 μM (*x* axis). A Ca^{2+}-selective electrode (Orion) was used to check the $[Ca^{2+}]$ and to measure the small increases upon adding 2 mM $MgCl_2$ to aliquots of the same buffers. With 0 mM Mg (●) the K_d was 46 nM for quin2 and 79 nM for fura2. With 2 mM Mg (○) the K_d was 89 nM for quin2 and 115 nM for fura2. The 2.5 μM quin2 or 0.25 μM fura2 are not expected to alter the free Ca^{2+} set by the 400–4000 times greater EGTA concentration. Lines were drawn with a fourth order least-squares fit program. These [D]'s should be similar to those after lysing a 1% (vol/vol) suspension of ghosts containing 250 or 25 μM quin2 or fura2 (fluorescences roughly comparable to Fig. 2 *A, inset*). The calibration curves are representative of three different experiments for each dye.

date, DIDS, EGTA, EDTA, HEPES, and Triton X-100 were purchased from Sigma Chemical Co. (St. Louis, MO). DIDS is 4,4′-diisothiocyanatostilbene-2,2′-disulfonic acid. EDTA is ethylenediaminetetraacetic acid. EGTA is ethyleneglycol-*bis*-(β-aminoethylether)-*N,N,N′,N* ′-tetraacetic acid. Fura2 is 1-[2-(5-carboxy-oxazol-2-yl)-6-aminobenzofuran-5-oxy]-2-(2′-amino-5′-methylphenoxy)-ethane-*N,N,N′,N*-tetraacetic acid. HEPES is *N*-2-hydroxyethylpiperazine-*N*′-2-ethane sulfonic acid. TPEN is *N,N,N′,N*′-tetrakis-(2-pyridylmethyl)ethylenediamine. Quin2 is 2-[[2-[*bis*(carboxymethyl)-amino]-5-methyl-phenoxy]-methyl]-6-methoxy-8-[*bis*(carboxymethyl)amino] quinoline.

RESULTS

Comparison of Active Transport in Quin2- and Fura2-loaded Ghosts

For an ion to be actively transported, it must be moved against an electrochemical gradient. In these experiments, $[Ca]_o$ was 1 mM. The ghost extruded Ca^{2+} to a steady-state $[Ca_{free}]_i$ of 100 nM and routinely produced a 10^4-fold gradient for Ca^{2+}. The fluorescence changes are the net result of active efflux and passive influx under normal physiological conditions.

The intracellular [D] was kept as low as possible to keep the buffering effects to a minimum without compromising the precision of the fluorescence detection. Because fura2 has a 30-fold greater fluorescence quantum yield than quin2 (Grynkiewicz et al., 1985), ghosts loaded with 10 times less fura2 (25 μM) fluoresced more intensely than those loaded with 250 μM quin2 (Fig. 2 *A*, *inset*). When normalized, the changes of the fluorescence with time were remarkably similar despite the 10-fold differences in [D] (Fig. 2 *A*). The initial fluorescence of Ca-loaded active ghosts remained high for 1–2 min until the Ca^{2+} pump lowered the $[Ca_{free}]_i$ below the saturation level of the dyes (Fig. 2 *A*). The decline of $[Ca_{free}]_i$ was parallel but shifted later in time by ~2 min in fura2-loaded ghosts because the initial $[Ca_{free}]_i$ was higher in ghosts with less chelator when the same initial $[Ca_{total}]_i$ was added during loading (Fig. 2 *B*). The fluorescence level of the ghosts fell until the pump reduced the $[Ca_{total}]_i$ such that $[Ca_{free}]_i$ was at the steady-state level of 60–100 nM; at this level the rate of influx equaled the rate of efflux. $d[Ca_{free}]_i/dt$ increased nonlinearly as a function of $[Ca_{free}]_i$ and was approximately equal at any $[Ca_{free}]_i$ for quin2- or fura2-loaded ghosts (Fig. 2 *B*, *inset;* also, 5 or 50 μM fura2 in Fig. 8 *B*). This was remarkable because, over the same time period, the change in $[Ca_{total}]_i$ over the same range of $[Ca_{free}]_i$ was more than eight times larger in ghosts with 250 μM quin2 compared with 25 μM fura2 (127.3 vs. 14.6 μM; Δ Ca^{2+} marked by dotted vertical lines in Fig. 2 *C*). This comparison was made from 150 to 600 s where both dyes were below saturation or in their sensitive ranges. As a consequence, $d[Ca_{total}]_i/dt$ as a function of $[Ca_{free}]_i$ was faster in quin2-loaded ghosts (Fig. 2 *C, inset*), which was not expected. These curves were hyperbolic and three times greater in magnitude at 1 μM $[Ca_{free}]_i$ with 10 times greater [D]. Therefore $d[Ca_{total}]_i/dt$ was not a direct function of $[Ca_{free}]_i$; i.e., the greater the [D], the higher the $d[Ca_{total}]_i/dt$, indicating that these chelators stimulate transport. The apparent upper limit of $d[Ca_{total}]_i/dt$ at $[Ca_{free}]_i > 500$ nM (five times the K_d for the dyes) does not indicate maximal transport nor saturation of the pump at 500 nM $[Ca_{free}]_i$. Instead it reflects the fact that $[Ca_{total}]_i$ changes little when the dyes are >95% saturated with Ca^{2+} while $[Ca_{free}]_i$ is changing greatly. This is also true for the saturation of CaM and fura2 in Fig. 3 *D*.

Active Transport Monitored by the Fura2 Ratio Method

The time course of Ca^{2+} transport monitored by the ratio method (Figs. 3 and 5) was similar to the rate observed using the original method (Figs. 2 and 4). The ratio of the fluorescent intensities at 340 and 380 nm is independent of photobleaching and other artifacts (Grynkiewicz et al., 1985). The fluorescence at 380 nm increases as the fluorescence at 340 nm decreases when $[Ca_{free}]_i$ is lowered due to active transport (Fig. 3 *A*). Fura2 responds to Ca^{2+} in ghosts precisely as predicted from calibration

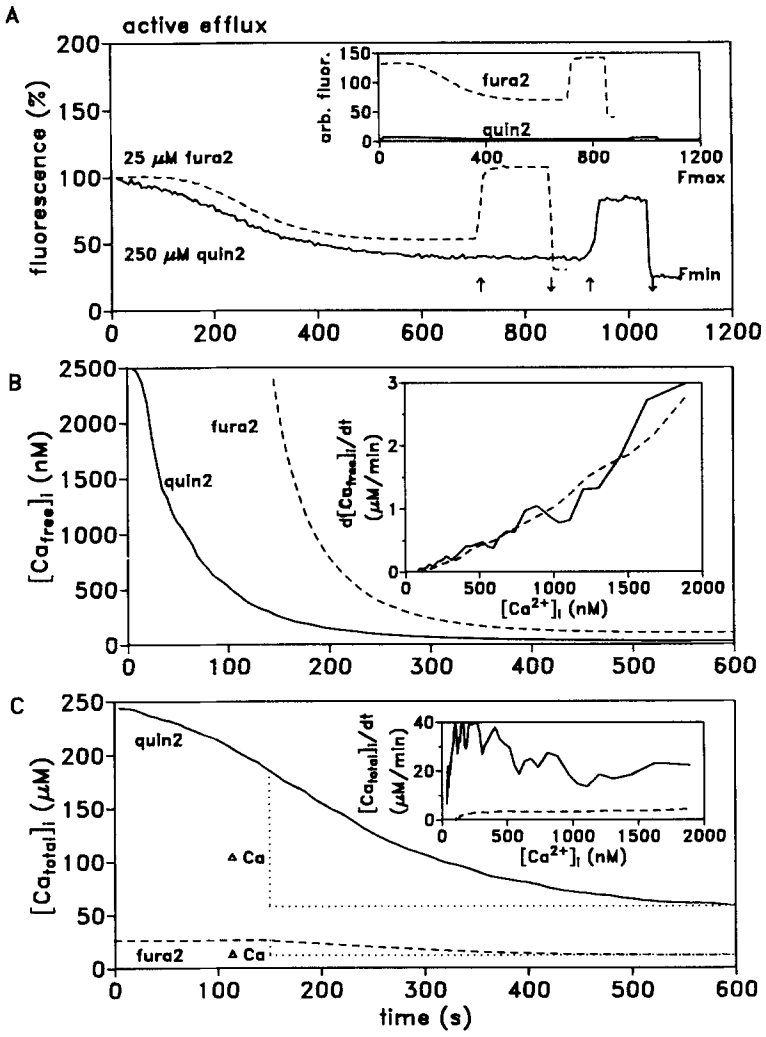

FIGURE 2. Comparison of the time course of net Ca^{2+} extrusion in quin2-(*solid line*) or fura2-(*dashed line*) loaded ghosts. Active ghosts were loaded with 10 times less fura2 (25 μM) than quin2 (250 μM). (*A*) Results normalized to $F_{initial}$ = 100% or approximately equal to F_{max}. F_{max} (↑) was determined with 0.02% Triton X-100 and F_{min} (↓) was determined by adding 4 mM EGTA and 50 mM Tris, pH 8.9 (final pH 8.3). After lysis with Triton X-100, F_{max} is higher for fura2 and lower for quin2 than $F_{initial}$ because the higher free Mg^{2+} concentration in the medium (2 mM in the medium with no ATP) increases the fluorescence of fura2 but decreases that of quin2 (see also Fig. 1). Under these conditions, $F_{initial}$ (Ca saturated conditions) rather than F_{max} was used for the calculations in Ca-loaded active ghosts. Ionomycin yields equal $F_{initial}$ and F_{max} (see Fig. 3). (*Inset*) Fluorescence before normalizing. Equal concentrations of the two dyes could not easily be compared because 250 μM fura2 was too intense to monitor at normal fluorometer gain and <250 μM quin2 was too low to be detected. (*B*) Conversion of the fluorescence values in *A* inset to $[Ca_{free}]_i$ vs. time. (*Inset*) $d[Ca_{free}]_i/dt$ vs. $[Ca_{free}]_i$. $d[Ca_{free}]_i/dt$ determined from ghosts with low (noisy) fluorescence levels (quin2) are more scattered. (*C*) $[Ca_{total}]_i$ vs. time calculated from *B*. Note that the early flat region of $[Ca_{total}]_i$ in the fura2 ghosts is only due to the saturation of the dye and the actual $[Ca_{total}]_i$ would be expected to be higher than this but unmeasurable by this method. (*Inset*) $d[Ca_{total}]_i/dt$ as a function of $[Ca_{free}]_i$. Apparent maximum of $d[Ca_{total}]_i/dt$ actually reflects dye saturation.

solutions; i.e., its properties are unaltered in the presence of membranes (see Materials and Methods).

Identifying Characteristics of the Active Transport

The extrusion of Ca^{2+} against a 10^4-fold concentration gradient ($[Ca]_o$ = 1 mM) must be due to the ATP-driven Ca^{2+} pump. Without ATP, active extrusion did not occur;

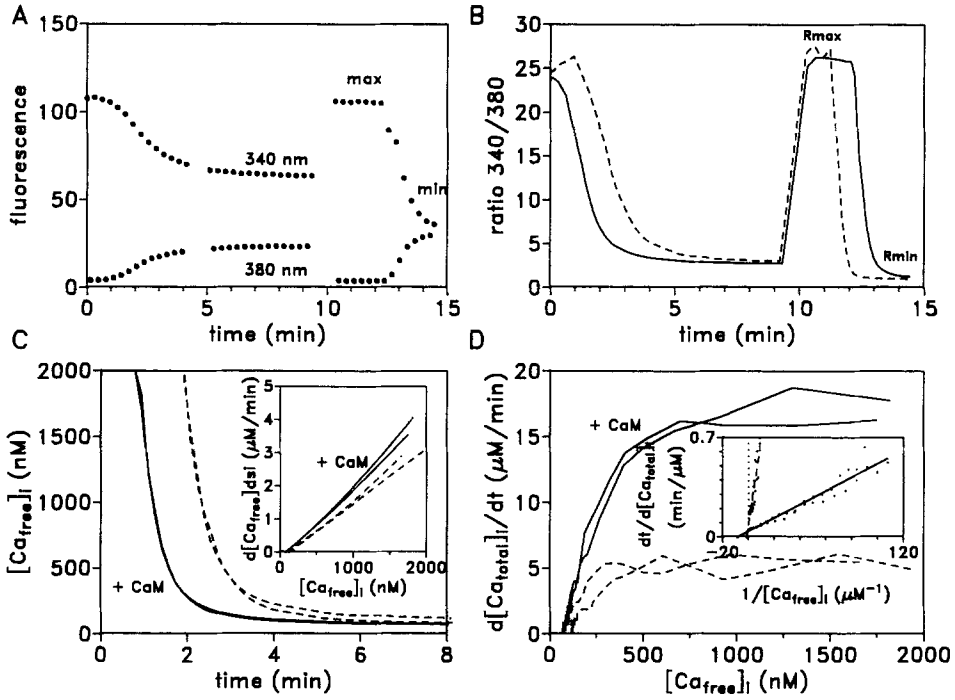

FIGURE 3. Ca^{2+} transport in active (ATP regenerating system) ghosts loaded with 25 μM fura2, and 0.25 mM $CaCl_2$ monitored by the ratio method during transport. Ghosts were loaded with (*solid line*) or without 5 μM CaM (*dashed line*). (*A*) Fluorescence measurements of ghosts loaded with 5 μM CaM at 340 and 380 nm. R_{max} was determined by adding 2 μM ionomycin. R_{min} was determined as usual. (*B*) The ratios obtained in ghosts with or without 5 μM CaM. (*C*) $[Ca_{free}]_i$ vs. time. (*C*) *Inset*, $d[Ca_{free}]_i/dt$ as a function of $[Ca_{free}]_i$. Two samples with 5 μM CaM (*solid line*) and two without (*dashed line*) are plotted. Similar stimulation by CaM was apparent in four other samples from the same preparation using the single wavelength method and in eight other experiments using the ratio method. (*D*) $d[Ca_{total}]_i/dt$ as a function of $[Ca_{free}]_i$ for the same data showing an increase in total extruded Ca^{2+} stimulated by 5 μM CaM at all $[Ca_{free}]_i$ above the steady-state level. (*D*) *Inset*, Lineweaver-Burk plot of $1/d[Ca_{total}]_i/dt$ as a function of $1/[Ca_{free}]_i$ for control ghosts and those loaded with 5 μM CaM.

the fluorescence of Ca-loaded passive ghosts remained at F_{max} (or R_{max}). Although there was a Na gradient across the membrane, this did not support extrusion in human red cells, in agreement with previous reports (Schatzmann, 1975). Without the regenerating system, 2 mM ATP was sufficient to maintain the transport for

10–20 min. However, ghosts with the regenerating system transported more rapidly than those without it, probably because ATP maintained at millimolar concentrations has an allosteric stimulatory effect (Rega, 1986*a*). With 0.5, 1, or 2 mM ATP, stabilized with the regenerating system, the steady-state $[Ca_{free}]_i$ was 80 nM and the $d[Ca_{free}]_i/dt$ at any $[Ca_{free}]_i$ was similar. ATP at 0.1 or 0.2 mM appeared to limit the rate of transport, and the steady-state $[Ca_{free}]_i$ was ~200 nM. Ghosts loaded with ATP but without Mg^{2+} transported very slowly. $LaCl_3$ (10 μM) or vanadate (200 μM) rapidly inhibited the transport when added to the medium; i.e., the fluorescence remained near maximal levels. The integrity of the ghosts was demonstrated by the fact that La^{3+}, added to the medium, could not enter the ghosts since this would quench the fluorescence.

Stimulation of Active Ca^{2+} Extrusion by Calmodulin

$d[Ca_{free}]_i/dt$ increased when the physiological concentration of CaM (5 μM) (Vincenzi et al., 1980; Foder and Scharff, 1981) was incorporated (Fig. 3 *C*). Smaller increases in $d[Ca_{free}]_i/dt$ in ghosts loaded with 10 and 100 nM CaM were also observed. The length of the initial plateau was much shorter in ghosts with CaM (Fig. 3, *B* and *C*). This indicated that at higher $[Ca_{free}]_i$, probably even during resealing, CaM stimulated the pump to lower $[Ca_{free}]_i$ more quickly. However, the shorter plateau may also be due to the extra chelating action of CaM which initially reduces $[Ca_{free}]_i$. The steady-state level of $[Ca_{free}]_i$ in CaM-loaded ghosts was ~20–30 nM lower than in the controls (Fig. 3 *C*), which implies that CaM can stimulate the pump even at 50–80 nM $[Ca_{free}]_i$. The stimulation of $d[Ca_{free}]_i/dt$ by CaM was apparent at all $[Ca_{free}]_i$, but, for example, the 25% increase at 1 μM $[Ca_{free}]_i$ (Fig. 3 *C, inset*) was less than the degree of stimulation observed in ATPase assays (Foder and Scharff, 1981; Muallem and Karlish, 1982; Rega, 1986*a*). But these comparisons of $d[Ca_{free}]_i/dt$ did not take into account the chelating capacity of CaM. When $d[Ca_{total}]_i/dt$ was calculated, a threefold stimulation by CaM was observed at 1 μM $[Ca_{free}]_i$ (Fig. 3 *D*). A Lineweaver-Burk plot of the data in Fig. 3 *D* with 25 μM fura2 and 5 μM CaM in the ghosts, CaM increased V_{max} (i.e., maximal $d[Ca_{total}]_i/dt$) from 13.4 to 24.8 μM/min and decreased K_m from 829 to 119 nM. However, the K_m and V_{max} values depend on whether $d[Ca_{free}]_i/dt$ or $d[Ca_{total}]_i/dt$ is used to determine K_m and V_{max} (see results and discussion of Fig. 6). Factors affecting the kinetics of CaM activation of the Ca pump will be addressed in greater detail in a subsequent paper.

Effect of $[Ca]_o$ and [D] on Passive Influx

Passive and active ghosts were studied since any factor that increased passive influx could be misinterpreted as inhibition of active extrusion. The magnitude of the influx opposing the active extrusion of Ca^{2+} was analyzed in Ca-depleted passive ghosts (without ATP). In quin2-loaded passive ghosts, $[Ca_{free}]_i$ increased slowly after adding 1 mM $[Ca]_o$ (Fig. 4 *A*). However, the $[Ca_{free}]_i$ at any time after adding $[Ca]_o$ rose more quickly in fura2 ghosts containing less [D]. Therefore, the low $-d[Ca_{free}]_i/dt$ (minus sign denotes influx) was partially due to chelation of the Ca^{2+} that entered as well as the low permeability of the ghosts to Ca^{2+} (cf. Fig. 4, *A* and *B*). The initial $-d[Ca_{free}]_i/dt$ increased as a function of increasing $[Ca]_o$ but decreased as [D] was increased (Fig. 4 *C*), which was strikingly different than observed in active ghosts. The

$[Ca_{free}]_i$ increased biphasically: initially faster and then slower with time after Ca^{2+} addition (Fig. 4, *A* and *B*, and Fig. 5, *A* and *C*). A similar biphasic influx was reported in ATP-depleted intact red cells (Schatzmann, 1973; Ferreira and Lew, 1977). Leaky ghosts do not account for the early fast phase since they do not retain the dye. The Ca-depleted ghosts are probably hyperpermeable and regain their normal low permeability as Ca^{2+} binds to the inner and outer surfaces of the membrane. Incidentally, the Ca buffering capacity of the membranes themselves would be equal in the influx and efflux experiments. Therefore, the membranes cannot account for

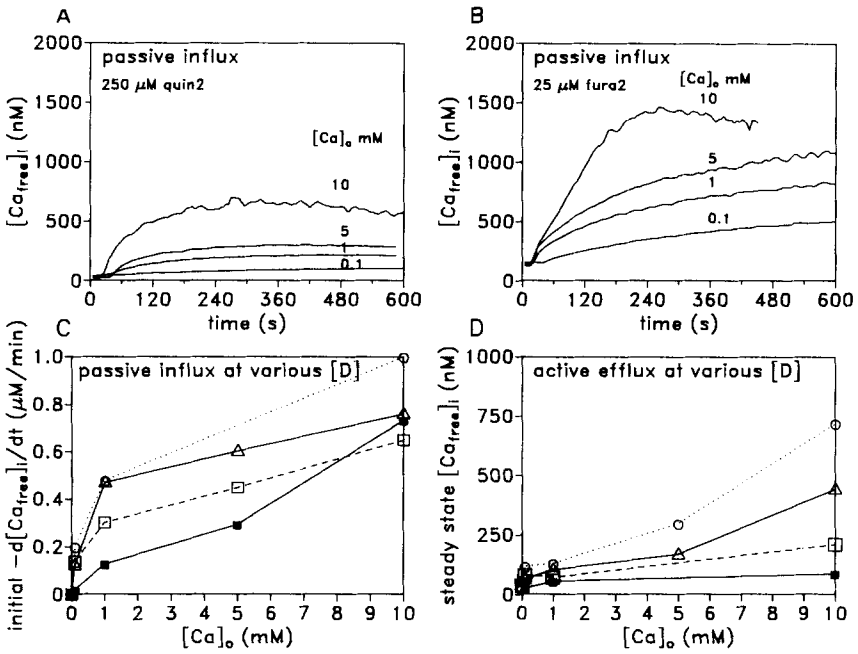

FIGURE 4. The effect of $[Ca]_o$ and [D] on $[Ca_{free}]_i$ in passive and active ghosts. The passive increase in $[Ca_{free}]_i$ in ghosts, prepared simultaneously from the same donor with 250 μM quin2 (*A*) or 25 μM fura2 (*B*) is plotted as a function of time. Ghosts were loaded and washed without Ca^{2+} in the medium. $[Ca]_o$ was added at the concentrations indicated on the traces after 30 s. (*C*) The initial maximum $-d[Ca_{free}]_i/dt$ (inward) is a function of $[Ca]_o$ and [D]. The dye concentrations were 5 (○), 25 (△), and 50 μM (□) fura2 and 250 μM quin2 (■) (*D*) The steady-state level of $[Ca_{free}]_i$ in active ghosts with varying [D], as indicated in the figure, as a function of increasing $[Ca]_o$. The [D]'s are marked by the same symbols and line types as in *C*.

the lack of differences observed between the $d[Ca_{free}]_i/dt$ in actively extruding ghosts with different [D] since differences in $d[Ca_{free}]_i/dt$ were observed during passive influx into ghosts with different [D].

The Effect of $[Ca]_o$ and [D] on Active Efflux

In contrast to passive transport, the $d[Ca_{free}]_i/dt$ of active ghosts is less sensitive to $[Ca]_o$ and almost completely insensitive to chelator [D]. Ca-loaded active ghosts

containing 5–250 μM dye were diluted in buffers with varying $[Ca]_o$ (0–10 mM) and the pump extrusion was monitored until steady-state $[Ca_{free}]_i$ was reached (Fig. 4 *D*). With 0–1 mM $[Ca]_o$ there was less than a twofold difference in the steady-state $[Ca_{free}]_i$ over a 50-fold range of [D] (Fig. 4 *D*). With 5–10 mM $[Ca]_o$ active ghosts could produce a 10^5-fold gradient for $[Ca_{free}]_i$ if 250 μM quin2 was incorporated, but only a

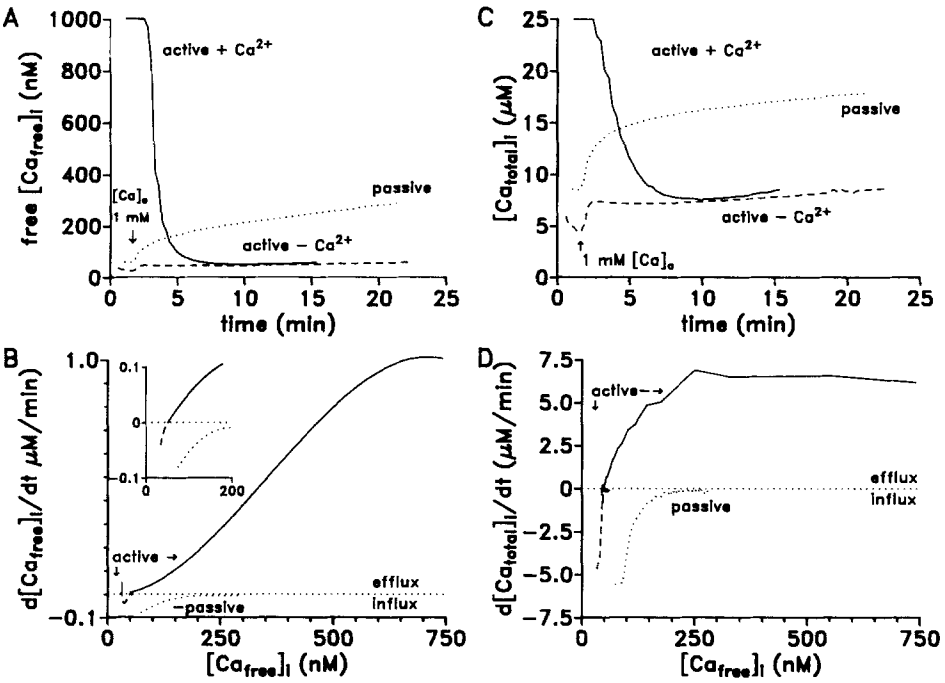

FIGURE 5. Comparison of the rates of change of free and total Ca during net efflux and influx in active ghosts and during net influx in passive ghosts. (*A*) Time course (ratio method) of net extrusion from Ca-loaded active ghosts (*solid line*) or influx into Ca-depleted active ghosts (*dashed line*). Ghosts were loaded with 25 μM fura2 and 10 nM CaM. These fluxes are compared with those in passive ghosts without ATP (*dotted line*) in which no steady-state level is reached. For influx studies active and passive ghosts were not loaded with Ca and were washed in Ca-free medium. Note that the initial $[Ca_{free}]_i$ is usually lower in the active ghosts and falls when warmed in Ca-free medium until 1 mM $CaCl_2$ is added to the medium. (*B*) Data in *A* converted to $d[Ca_{free}]_i/dt$ as a function of $[Ca_{free}]_i$ in Ca-loaded (efflux) or Ca-depleted (influx) active ghosts or Ca-depleted passive ghosts (influx). (*Inset*) Expansion of the flux rates below 200 nM. (*C*) The same data as in *A* expressed as $[Ca_{total}]_i$. (*D*) The results in *C* calculated as $d[Ca_{total}]_i/dt$ vs. $[Ca_{free}]_i$.

10^4-fold gradient if 5 μM fura2 was incorporated. $d[Ca_{free}]_i/dt$ as a function of $[Ca_{free}]_i$ was similar in medium containing 0, 0.1, or 1 mM $[Ca]_o$, but slower in medium containing 5 and 10 mM $[Ca]_o$, especially in ghosts with lower [D] (data not shown). Either high $[Ca]_o$ inhibits the pump (K_i = 9 mM; Rega, 1986*a*) or the increased rate of passive influx appears as an inhibition of the pump. The latter would be especially apparent in ghosts with lower [D] to buffer the influx.

Comparison of Net Extrusion and Influx in Active and Passive Ghosts

For efflux and influx experiments $d[Ca_{free}]_i/dt$ and $d[Ca_{total}]_i/dt$ were compared in ghosts loaded under passive (no ATP) and active conditions (ATP-regenerating system) with or without Ca^{2+} (Fig. 5). An important observation from this experiment was that the same steady-state level of 80 nM $[Ca_{free}]_i$ was approached from either high or low initial $[Ca_{free}]_i$ in active ghosts (Fig. 5 *A*). Therefore the steady-state $[Ca_{free}]_i$ was set by the sensitivity of the pump to $[Ca_{free}]_i$ and was not influenced by the $[Ca_{free}]_i$ and [D] incorporated during loading.

The rate of net gain of $[Ca_{free}]_i$ ($-d[Ca_{free}]_i/dt$) was slower in active than in passive Ca-depleted ghosts. After adding 1 mM $[Ca]_o$ to active ghosts, the rate of influx exceeded the rate of active efflux only briefly. After 1 min the efflux equaled the influx and $d[Ca_{free}]_i/dt$ became 0 at a steady-state level of 80 nM (Fig. 5 *B*). In contrast, no steady-state level was attained in passive ghosts. The values for $-d[Ca_{free}]_i/dt$ at $[Ca_{free}]_i > 200$ nM were negligible in passive ghosts compared with those for $d[Ca_{free}]_i/dt$ in Ca^{2+}-loaded active ghosts (Fig. 5 *B*). Therefore, above 200 nM $[Ca_{free}]_i$, $d[Ca_{free}]_i/dt$ is mainly due to pump activity and can be used as a monitor of pump rate for kinetic analysis in Ca-loaded active ghosts (see Fig. 6).

When $[Ca_{free}]_i$ (Fig. 5 *A*) was converted to $[Ca_{total}]_i$ (Fig. 5 *C*), the Ca^{2+} influx was revealed to be quite substantial but still less than the efflux. Again $d[Ca_{total}]_i/dt$ (Fig. 5 *D*) was a hyperbolic function from 50 to 250 nM $[Ca_{free}]_i$ (as in Fig. 2 *C*, *inset*). The net passive influx in active ghosts was negligible when $[Ca_{free}]_i$ was between 50 and 250 nM. Therefore this range was used for kinetic analysis (Fig. 6 *B*).

Kinetic Analysis of Active Ca^{2+} Transport Monitored with Different [D]

To determine whether the [D] had any effect on the K_m or V_{max}, data from the insets of Fig. 2, *B* and *C*, were compared on Lineweaver-Burk plots (Fig. 6, *A* and *B*). The K_m and V_{max} were determined from $d[Ca_{free}]_i/dt$ and $d[Ca_{total}]_i/dt$ ($K_{m\text{-}free}$, $V_{max\text{-}free}$, $K_{m\text{-}total}$, and $V_{max\text{-}total}$, respectively). The plots of $dt/d[Ca_{free}]_i$ vs. $1/[Ca_{free}]_i$ (Fig. 6 *A*) were not linear and did not have a positive *y* intercept. The reciprocal rates became linear as a second-order function ($1/[Ca_{free}]_i^2$) and the intercepts yielded a $V_{max\text{-}free}$ of 1.52 μM/min and a $K_{m\ free}$ of 790 nM for the high affinity mode of the pump. Using $V_{max\text{-}free}$, the Hill coefficient was 1.93, which suggests that the binding of Ca^{2+} may promote the binding of another Ca^{2+} or Ca^{2+} complex to activate the pump (Lew et al., 1982*b*; Villalobo et al., 1986).

The Lineweaver-Burk plots of $1/d[Ca_{total}]_i/dt$ as a function of $1/[Ca_{free}]_i$ in quin2- and fura2-loaded ghosts were linear but not superimposable (Fig. 6 *B*). There was at least a fivefold increase in the $V_{max\text{-}total}$ values (10.3 to 52.9 μM/min) and a fivefold decrease in the $K_{m\ total}$ values (638 and 115 nM) with a tenfold increase in [D]. Both $K_{m\ total}$ values were lower and both $V_{max\ total}$ values were higher than those determined from $d[Ca_{free}]_i/dt$ (compare Fig. 6 *A*, *inset*, and Fig. 6 *B*). When $V_{max\text{-}total}$ was used to calculate the Hill plot, the Hill coefficients were close to 1, indicating that pump rate was a first order function of [CaD]. More notably, with different [D] the reciprocals of $d[Ca_{total}]_i/dt$ could be plotted on the same line as a function of $1/[Ca_{total}]_i$ (Fig. 6 *B*, *inset*). Several experimental observations have led us to speculate that $d[Ca_{total}]_i/dt$ was a function of [CaD] or [Ca chelator] as well as a function of $[Ca_{free}]_i$; for example, in

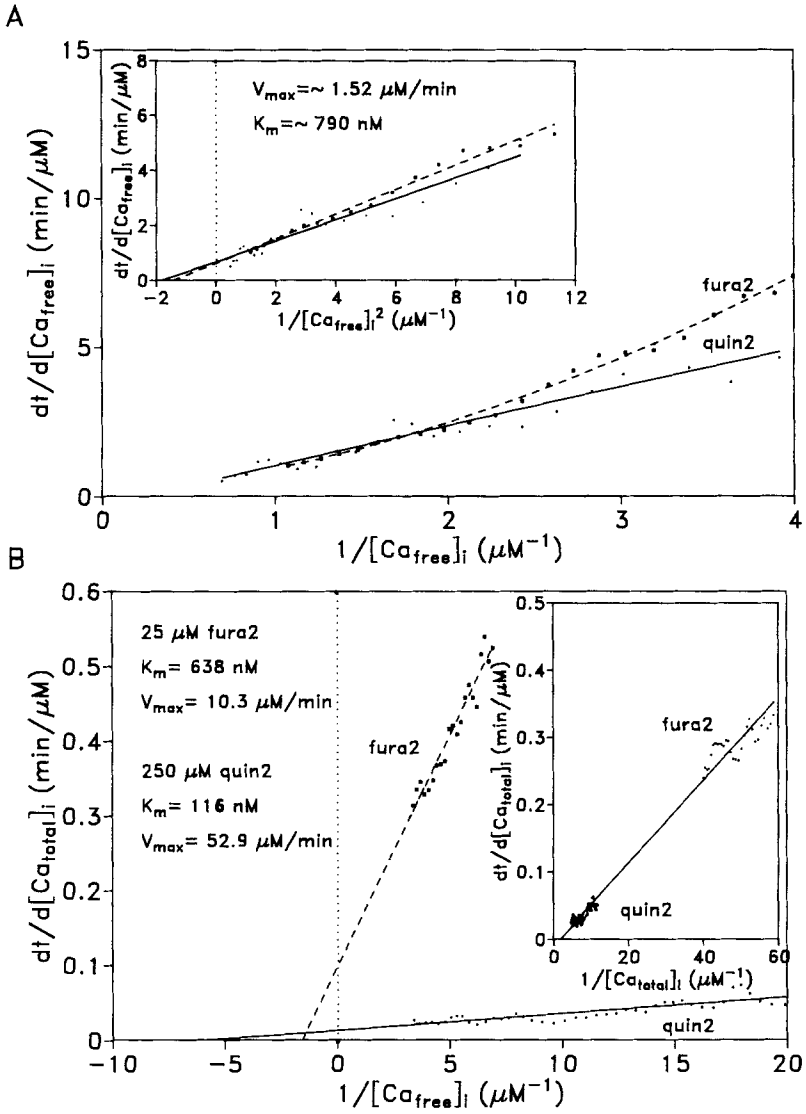

FIGURE 6. Lineweaver-Burk plots of the rates of change of $[Ca_{free}]_i$ (*A*) and $[Ca_{total}]_i$ (*B*) in active ghosts loaded with either 250 μM quin2 (*solid line*) or 25 μM fura2 (*dashed line*). Data are replotted from Fig. 2 *B* (*inset*). The reciprocal rates $dt/d[Ca_{free}]_i$ (*A*) and $dt/d[Ca_{total}]_i$ (*B*) are plotted as functions of $1/[Ca_{free}]_i$. In *A* (*inset*) the $dt/d[Ca_{free}]_i$ is a linear function of $1/[Ca_{free}]_i^2$. In *B* (*inset*) the $dt/d[Ca_{total}]_i$ is plotted as a function of $1/[Ca_{total}]_i$. Only the values for $[Ca_{free}]_i$ between 250 nM and 1 μM and for $[Ca_{total}]_i$ between 100 and 500 nM were used because these ranges were unaffected by passive influx or dye saturation. $dt/d[Ca_{free}]_i$ was linear as a function of $1/[Ca_{free}]_i^2$ (*inset*) but not $1/[Ca_{free}]_i$. $dt/d[Ca_{total}]_i$ was linear as a function of $1/[Ca_{free}]_i$ but this function was very different for each [D]. $dt/d[Ca_{total}]_i$ is a linear function of $1/[Ca_{total}]_i$ but is dependent on the [D] as well as the pump activity.

ghosts with 5, 25, 50, or 250 μM dye (Fig. 8, *A* and *B*) or with 25 μM fura2 plus 0.2 mM EGTA or 1 mM EGTA (Fig. 7 *D*). These observations will be explained further in the Discussion section. [CaD] is a function of the pump activity as well as total [D] incorporated during resealing. $d[Ca_{total}]_i/dt$ was not an independent indication of Ca^{2+} pump activity. $K_{m\ total}$ or $V_{max\ total}$ were not strictly characteristics only of the pump activity since the affinity and rate increased with [D]. And yet to demonstrate the extent of the stimulation by CaM (Fig. 3 *D*), $d[Ca_{total}]_i/dt$ must be compared.

DISCUSSION

Ca chelators have been used in most Ca^{2+} transport assays in ghosts, often at high concentrations (1–10 mM), to set a series of stable $[Ca_{free}]_i$ between 1 and 100 μM (Schatzmann, 1973; Quist and Roufogalis, 1975; Lew et al., 1982*b*; Kratje et al., 1983). With quin2 or fura2 in active ghosts, stable buffering is neither required nor desirable; the Ca^{2+} pump creates a spectrum of $[Ca_{free}]_i$ below 2.5 μM to 50 nM, which can be monitored "on line" every second. However, with either type of approach, $d[Ca_{total}]_i/dt$ would be expected to be comparable at any $[Ca_{free}]_i$. When quin2 was replaced by fura2, it was at first reassuring that the time course of the fluorescence signal and consequently $d[Ca_{free}]_i/dt$ was not altered despite the 10-fold reduction in Ca buffering capacity. However, on closer examination, this new method for monitoring transport revealed an enigma. Over the same range of $[Ca_{free}]_i$, there was 10 times less $[Ca_{total}]_i$ to be transported to reach the same steady-state $[Ca_{free}]_i$ in ghosts loaded with 10 times less dye. Intuitively, this should occur 10 times faster; i.e., $d[Ca_{free}]_i/dt$ should have been increased as the buffering capacity was reduced. However, clearly $d[Ca_{free}]_i/dt$ was unaltered; instead $d[Ca_{total}]_i/dt$ was reduced in ghosts with less [D].

Since the dyes are specialized Ca chelators, we began to wonder whether the transport rates, reported by a number of investigators, also increase as a function of the chelator concentration when compared at ~5 μM $[Ca_{free}]_i$ (Fig. 7). Although Fig. 7 *A* certainly shows this trend, it should be kept in mind that these were performed under somewhat different experimental conditions. This paradoxical "EGTA effect" on the rate of transport (Al-jobore and Roufogalis, 1981; Kotogal et al., 1983; Rega, 1986*b*) may be common to all Ca^{2+} chelators, including the new fluorescent dyes. Whether this effect is completely nonspecific or whether some chelators are more effective than others is not apparent from the data available at this time.

At first the discrepancies between Ca^{2+} pump properties from membranes prepared and assayed with and without Ca-EGTA were explained by protection from trace metals or removal of membrane regulator substances. But Sarkadi et al. (1979) realized that these could not explain the increased rate of Ca^{2+} transport in a preparation of inside-out vesicles when the $[Ca_{free}]_i$ was kept constant while the [EGTA] and $[Ca_{total}]_i$ were increased (Fig. 7 *B*). They proposed that the Ca-EGTA complex could bind to the pump and activate it; the Ca^{2+} would be transported but the EGTA would not. EGTA also activates the plasma membrane Ca-ATPase activity (Al-jobore and Roufogalis, 1981) and the Ca^{2+} uptake into plasma membrane preparations (Al-jobore and Roufogalis, 1981; Kotogal et al., 1983). This activation concurs with the idea that any negatively charged molecule with a hydrophobic

moiety, e.g., CaM, acidic phospholipids (Niggli et al., 1981), or Ca chelators, may activate the pump.

It appears that this phenomenon also occurs with Ca-quin2 and Ca-fura2. To further test this observation, ghosts were loaded with 0.2 mM EGTA or 1 mM EGTA in addition to 25 μM fura2 (Fig. 7 *D*). The $d[Ca_{free}]_i/dt$ as a function of $[Ca_{free}]_i$ in ghosts with EGTA was superimposable with those from ghosts loaded with 25 μM fura2 alone (Fig. 7 *D*). Consequently, the $d[Ca_{total}]_i/dt$ at 1 μM $[Ca_{free}]_i$ was much faster

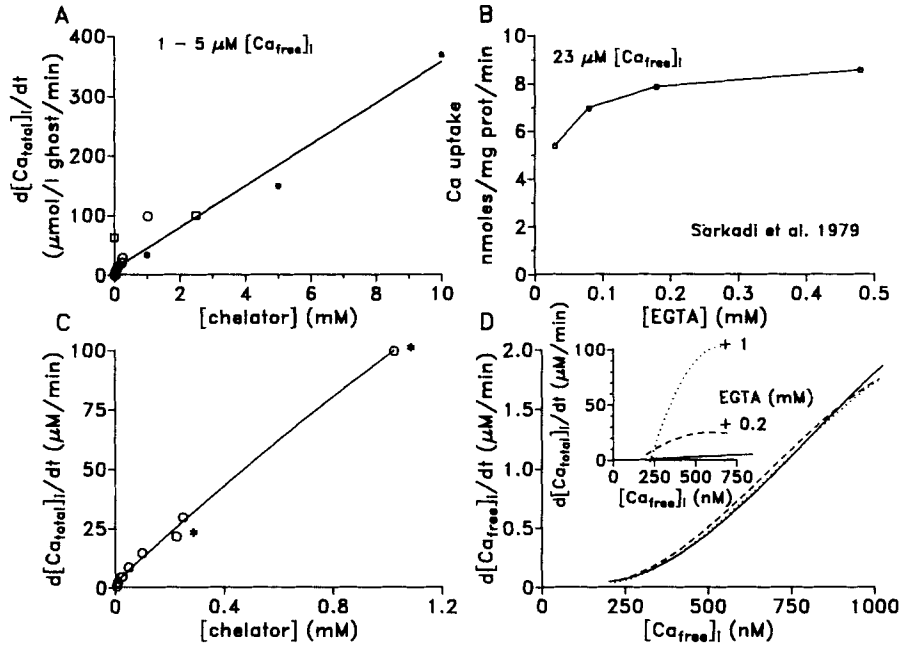

FIGURE 7. (*A*) A plot of increasing $[Ca_{total}]_i/dt$ in resealed ghosts as a function of the Ca^{2+} chelator concentration incorporated during resealing when $[Ca_{free}]_i$ was ~5 μM, 1 μM, or ~1 mM as indicated using data from published sources. Closed circles indicate data from Yingst and Hoffman (1978), 5 μM $[Ca_{free}]_i$ with 20 μM EGTA, 70 μM arsenazo III = 90 μM chelator total; Quist and Roufogalis (1975), at 5 μM $[Ca_{free}]_i$ with 1 mM EDTA; Schatzmann (1973), 5 μM $[Ca_{free}]_i$ with 5 mM EGTA; and Kratje et al. (1983), at 5 μM $[Ca_{free}]_i$ with 10 mM EDTA. Open circles indicate $d[Ca_{total}]_i/dt$ at 1 μM $[Ca_{free}]_i$ with 5, 10, 25, 50, and 100 μM fura2, 250 μM quin2, 25 μM fura2 plus 0.2 mM EGTA, or 25 μM fura2 plus 1 mM EGTA. These latter values are plotted separately in *C*. Open squares indicate transport rates when higher $[Ca_{free}]_i$ was used in the assays reported by Larsen et al. (1978) (1 mM $[Ca_{free}]_i$ with no chelator) and by Muallem and Karlish (1979) (1 mM $[Ca_{free}]_i$ with 2.5 mM HEDTA). Note that the units (micromolar per minute) determined by calculation of $d[Ca_{total}]_i/dt$ with fluorescent dyes are equivalent to micromolar per liter ghosts per minute determined in ^{45}Ca experiments. (*B*) The transport values from inside-out vesicles reported in Table 1 in Sarkadi et al. (1979) at 23 μM free Ca^{2+} concentration are plotted for increasing [EGTA] which correspond to total [Ca] (50, 100, 200, and 500 μM). (*D*) The $d[Ca_{free}]_i/dt$ as a function of $[Ca_{free}]_i$ for active ghosts loaded with 25 μM fura2 or with this concentration of dye plus 0.2 mM EGTA or 1 mM EGTA. The inset shows the calculated $d[Ca_{total}]_i/dt$ for these ghosts loaded with 25 μM fura2 alone or with 0.2 or 1 mM EGTA as labeled.

as a function of $[Ca_{free}]_i$ with higher chelator concentrations incorporated (Fig. 7 *D*, *inset*). These transport rates at similar values of $[Ca_{free}]_i$ were comparable to those reported using ^{45}Ca or arsenazo III when differences in chelator concentrations (EDTA, EGTA, HEDTA, fura2, quin2) were considered (Fig. 7 *A*).

In addition to free Ca^{2+}, the pump seems to accept complexed Ca^{2+} for transport, perhaps at a common nonselective binding site (Fig. 8 *C*). With quin2 and fura2, the

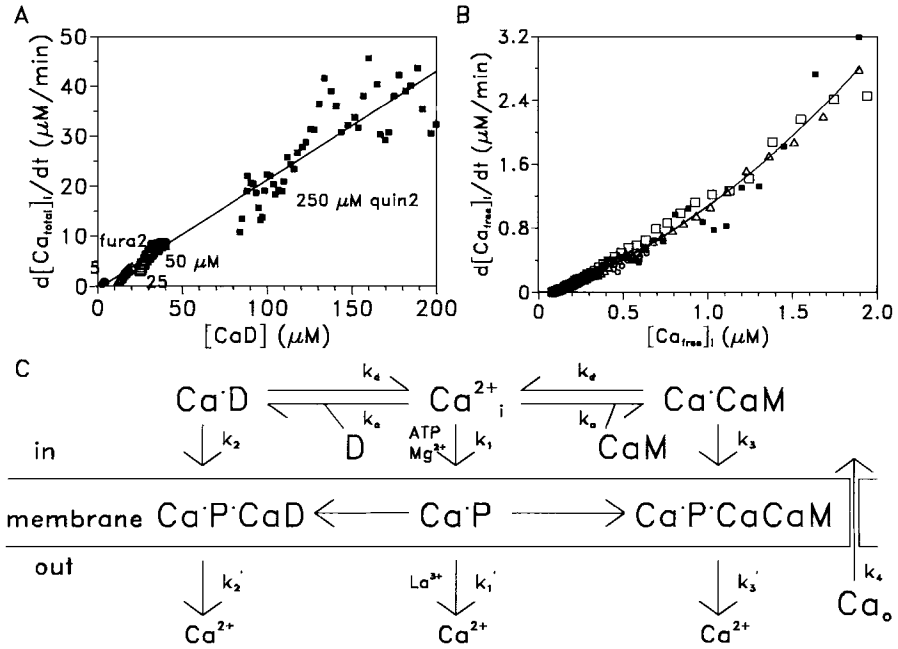

FIGURE 8. (*A*) $d[Ca_{total}]_i/dt$ was a linear function of the [CaD] when there was 5 (○), 25 (△), 50 (□), and 250 (■) μM [D] in the ghosts. The equation for the solid line is $d[Ca_{total}]_i/dt = 0.218\ min^{-1} \times [CaD]$. (*B*) $d[Ca_{free}]_i/dt$ is a function of $[Ca_{free}]_i$ independent of [D] and can be increased by CaM. (*C*) Scheme of the reactions affecting $[Ca_{free}]_i$ in active ghosts loaded with 1 mM Ca, calmodulin, and dyes. *P*, pump; *D*, dye; *CaD*, Ca-dye complex; *CaM*, calmodulin; *CaCaM*, Ca complex of CaM. The pump may bind Ca, CaD, or CaCaM with rate constants k_1, k_2, and k_3 to extrude Ca^{2+}. Note that in Ca-loaded active ghosts, association and dissociation rate constants for the dyes are too fast to be rate limiting (Quast et al., 1984; Jackson et al., 1987) ($K_a = 10^9$ and $5 \times 10^8\ M^{-1}s^{-1}$; $K_d = 84\ s^{-1}$ and $83\ s^{-1}$ for quin2 and fura2, respectively). For example, in ghosts loaded with 25 μM fura2 at 1 μM $[Ca_{free}]_i$, [CaD] is 22.42 μM, [D] is 2.58 μM, K_d is 4,980 min^{-1}, and K_a is $4.35 \times 10^4\ M^{-1}min^{-1}$, which makes the association and dissociation rates ~111,940 μM/min or 10^5 times faster than $d[Ca_{free}]_i/dt$ (1 μM/min) or $d[Ca_{total}]_i/dt$ (5 μM/min).

coordination of the transport modes with rate constants k_1, k_2, and k_3 appear to be under the control of $[Ca_{free}]_i$ (Fig. 8 *C*). As yet undetermined is whether the Ca:dye complex stimulates pumping at the low affinity Ca^{2+} regulatory site, at the Ca:[ATP] allosteric stimulatory site (Rega, 1986*a*), or at the CaM binding site (Kotogal et al.,

1983). The CaD complex does not stimulate transport once $[Ca_{free}]_i$ is below the steady-state level (cf. Fig. 8, *A* and *B*). This implies that CaCaM and CaD activate pumps that have Ca^{2+} bound to them but not free pumps. It should be kept in mind that our reported $[Ca_{total}]_i$ values are only calculated from the direct measurements of $[Ca_{free}]_i$ and are not a direct measurement of $[Ca_{total}]_i$ itself. However, direct measurements over the nanomolar range, even with chelators to increase the $[Ca_{total}]_i$, would be difficult to detect by atomic absorption spectrophotometry, especially with this time resolution or with easy differentiation of intracellular versus extracellular Ca and independent from artifacts of leaky ghosts.

Al-jobore and Roufogalis (1981) proposed that EGTA converted the low affinity state to a high affinity state of the enzyme to stimulate Ca^{2+} ATPase activity. A similar conversion from a low to a high affinity mode of the pump could be construed from the results in Fig. 6 *B* when the K_m was calculated from $d[Ca_{total}]_i/dt$ as a function of $[Ca_{free}]_i$ at higher chelator concentrations. But $d[Ca_{total}]_i/dt$ is not only a characteristic of the pump activity alone but secondarily a function of [D] added and $[Ca_{free}]_i$ resulting from pump activity. In our opinion, the K_m for the pump's affinity for $[Ca_{free}]_i$ should be calculated from $d[Ca_{free}]_i/dt$ because it is independent of [D].

Kotagal et al. (1983) demonstrated that the stimulation by CaM decreased as the EGTA concentration was increased and suggested that Ca-EGTA may mimic the activation by the Ca:CaM complex. We have observed that the stimulation by CaM is greater in ghosts loaded with 10 μM compared with 100 μM fura2 (data not shown; Zhu, Eichen, and James-Kracke, manuscript in preparation). Although frequently it is said that CaM stimulates transport, it has been clearly demonstrated that it is the Ca:CaM complex that stimulates pump activity (Foder and Scharff, 1981; Scharff and Foder, 1982; Scharff et al., 1983). In our experiments, there was one difference between the activation by the Ca-dye complex and CaCaM. Increasing the [D] 10-fold from 25 to 250 μM did not increase $d[Ca_{free}]_i/dt$ but increased $d[Ca_{total}]_i/dt$ 7-fold at 1 μM $[Ca_{free}]_i$. In contrast, 5 μM CaM, which increases the chelator concentration less than twofold, increased $d[Ca_{free}]_i/dt$ by 25%, but this was sufficient to increase $d[Ca_{total}]_i/dt$ threefold at 1 μM $[Ca_{free}]_i$ as observed in ATPase assays (Kotogal et al., 1983; Villalobo et al., 1986). These results may be showing us for the first time that Ca^{2+} passes directly from CaM out through the pump undetected by the dye as free Ca^{2+}. This is still somewhat speculative since this is the first method that yields results of this nature for which there is little other explanation.

These new ideas need to be discussed within the framework of observations indicating that mild trypsinization of the Ca pump, which removes the CaM binding domain, fully stimulates the ATPase activity (Taverna and Hanahan, 1980) and transport into inside-out vesicles (Sarkadi et al., 1987) in the absence of CaM. CaM has been postulated to displace an inhibitory portion of the pump (for review, see Carafoli, 1991). The CaM binding domain is flanked by two acidic groups which have been postulated to relay Ca to its high affinity binding site by acting as a "Ca filter" (Carafoli, 1991). Our transport method could not distinguish between a relay method in rapid series with the high affinity site or a parallel transport through a separate site directly from CaM. The relay method would presumably move Ca from CaM to the high affinity transport site without the Ca^{2+} ion passing through a dissociated free ion state. Trypsinization may expose these flanking Ca binding sites such that they

extrude Ca, or bind and relay Ca to the high affinity binding site in the absence of the CaCaM complex; i.e., CaM need not be present as long as these sites are exposed. It has been suggested that the CaEGTA complex, by virtue of being less bulky, can gain access to this site without CaM binding to displace the inhibitory component of the pump.

Our observations may also suggest a different interpretation for the cooperative nature of Ca binding to the pump. $[Ca_{free}]_i$ must be raised to the second power to best fit the data in Figs. 2 *B* (*inset*), 3 *D*, and 8 *B*. Lew et al. (1982*b*) reported that the efflux rate, in the low nanomolar range of the pump activity below steady state, was a function of $[Ca_{free}]_i^2$ (high affinity mode). They suggested that the pump was activated by the internal binding of two Ca^{2+} ions though both ions were not necessarily transported. In contrast, Kratje et al. (1983) reported no evidence for cooperativity when $d[Ca_{total}]_i/dt$ (with 10 mM EDTA) was plotted as a function of micromolar $[Ca_{free}]_i$ (low affinity mode). However, over the same range of $[Ca_{free}]_i$, in fura2-loaded ghosts, the linearity of the Lineweaver-Burk plot depends on whether $d[Ca_{free}]_i/dt$ or $d[Ca_{total}]_i/dt$ is plotted against $[Ca_{free}]_i$. The binding of Ca^{2+} to the pump and to the D or CaM to activate the pump may be the basis of the second power function we observed (see also Carafoli, 1991). The apparent cooperativity did not appear to be dependent on the presence of CaM, perhaps because the dyes also activate transport by a similar mechanism. Hill plots of the $d[Ca_{free}]_i/dt$ in ghosts with and without CaM from Fig. 3 *C* (*inset*) had slopes of 1.91. Villalobo et al. (1986) also observed a Hill coefficient of 2 in the absence of CaM with EGTA, and a variable coefficient with CaM increasing from 2 to 4 as the Mg concentration was raised from 2 to 5 mM.

In most other Ca^{2+} transport assays, $d[Ca_{free}]_i/dt$ cannot be monitored. Only $d[Ca_{total}]_i/dt$ is monitored as a function of $[Ca_{free}]_i$ and its dependence on the chelator concentration has largely been overlooked. A unique characteristic of the present method is that the $d[Ca_{free}]_i/dt$ could be monitored and, because the ghost contents are known, the $d[Ca_{total}]_i/dt$ could be calculated. Because of this, the effect of chelated forms of Ca^{2+} on transport activity is revealed for the first time. In other types of intact cells, loaded with the fluorescent dyes as the permeant acetoxy methyl ester, mainly $[Ca_{free}]_i$ is monitored and $[Ca_{total}]_i$ is not since the concentration of dye and cytosolic Ca buffers or sequestrated stores in organelles is not known. Only in the ghost model system are there no unknown cytosolic buffers or intracellular organelles to prevent this calculation. It is physiologically relevant to monitor $[Ca_{free}]_i$ and $d[Ca_{free}]_i/dt$ since these regulate cell activity. K_m and V_{max} determined from $d[Ca_{free}]_i/dt$ were independent of the [D] but traditionally K_m has been calculated from $d[Ca_{total}]_i/dt$. The physiological meaning of V_{max} calculated from $d[Ca_{free}]_i/dt$ is not quite clear but seems to be more characteristic of the pump than the very different $V_{max\ total}$ calculated from $d[Ca_{total}]_i/dt$, which seems to indicate the maximal pump rate under the influence of cytosolic Ca^{2+} buffers. Therefore, $d[Ca_{total}]_i/dt$ is not just an experimentally induced rate. These rates point out an interesting way that the cell can extrude a buffered load of intracellular Ca^{2+} more rapidly. Calmodulin and probably other soluble chelators in the cytoplasm can activate the pump (Rasmussen, 1989) since this activation seems to have minimal selectivity restrictions. This method of activation by cytosolic Ca^{2+} buffers would fit well the hysteretic activation of the Ca^{2+} pump described by Scharff et al. (1983). The latency in activation could be due to the

loading of cytosolic Ca^{2+} buffers and the subsequent stimulation would depend on the $[Ca_{free}]_i$ and the concentration of Ca-chelator complexes. The unusual observation that the Ca^{2+} pump rate is dependent not only on $[Ca_{free}]_i$ but also on the Ca^{2+} influx rate might also be explained by the rate of loading of intracellular chelator substances and pump activity stimulated by Ca complexes (Yang and Yingst, 1989). Our observations also agree with the proposal by Enyedi et al. (1987) that the maximal velocity and the calcium affinity of the red cell calcium pump are regulated independently. From our results V_{max} is a function of $d[Ca_{total}]_i/dt$ and K_m is a function of $d[Ca_{free}]_i/dt$.

In conclusion, the measurement of $d[Ca_{free}]_i/dt$ and $d[Ca_{total}]_i/dt$ in fura2-loaded active ghosts has led to new information about Ca^{2+} pump activity. The steady-state $[Ca_{free}]_i$ and pump activity in tightly resealed ghosts correlates well with the membrane transport properties of intact red cells. Over the nanomolar range of $[Ca_{free}]_i$, CaM greatly stimulates transport, seemingly by permitting the extrusion of the Ca^{2+} bound to the CaM while CaM is retained in the cell.

This project was begun at the SUNY Health Science Center in Syracuse, NY and continued in Columbia, MO. The technical assistance of J. Chai and J. Meacham, and more recently that of D. Johnson, I. Bozoky, and a graduate student, Y. Zhu, was greatly appreciated. Discussions with Drs. M. Milanick, J. Robinson, J. Freedman, and D. Yingst were very helpful.

This project was supported by the New York Affiliates of the American Heart Association/Mid-Hudson and Finger Lakes regions, the National American Heart Association, the NIH (AR-35435), the Muscular Dystrophy Association, the Research Foundation of the State University of New York, and Norwich Eaton Pharmaceuticals.

Original version received 22 June 1990 and accepted version received 24 September 1991.

REFERENCES

Al-jobore, A., and B. D. Roufogalis. 1981. Influence of EGTA on the apparent Ca^{2+} affinity of the Mg^{2+}-dependent, Ca stimulated ATPase in the human erythrocyte membrane. *Biochimica et Biophysica Acta.* 645:1–9.

Blinks, J. R., W. G. Wier, P. Hess, and F. G. Pendergast. 1982. Measurement of Ca^{2+} concentrations in living cells. *Progress in Biophysical and Molecular Biology.* 40:1–114.

Bond, G. H., and D. L. Clough. 1973. A soluble protein activator of (Mg^{2+} + Ca^{2+}) dependent ATPase in human red cell membranes. *Biochimica et Biophysica Acta.* 323:592–599.

Cantley, L. C., M. D. Resh, and G. Guidotti. 1978. Vanadate inhibits the red cell (Na^+, K^+)ATPase from the cytoplasmic side. *Nature.* 272:552–554.

Carafoli, E. 1991. Calcium pump of the plasma membrane. *Physiological Reviews.* 71:129–153.

David-Dufilho, M., T. Montenay-Garestier, and M. Devynck. 1988. Fluorescence measurements of free Ca^{2+} concentration in human erythrocytes using the Ca^{2+}-indicator fura-2. *Cell Calcium.* 9:167–179.

Enyedi, A., M. Flura, B. Sarkadi, G. Gardos, and E. Carafoli. 1987. The maximal velocity and the calcium affinity of the red cell calcium pump may be regulated independently. *Journal of Biological Chemistry.* 262:6425–6430.

Farrance, M. L., and F. P. Vincenzi. 1977. Enhancement of (Ca^{2+} + Mg^{2+})-ATPase activity of human erythrocyte membranes by hemolysis in isoosmotic imidazole buffer. II. Dependence on calcium and cytoplasmic activator. *Biochimica et Biophysica Acta.* 471:59–66.

Ferreira, H. G., and V. L. Lew. 1977. Passive Ca transport and cytoplasmic Ca buffering in intact red cells. *In* Membrane Transport in Red Cells. J. C. Ellory and V. L. Lew, editors. Academic Press, New York. 53–91.

Foder, B., and O. Scharff. 1981. Decrease of apparent calmodulin affinity of erythrocyte (Ca^{2+} + Mg^{2+})-ATPase at low Ca^{2+} concentrations. *Biochimica et Biophysica Acta.* 649:367–376.

Garrahan, P. J. 1986. Calmodulin and other physiological regulators of the Ca^{2+} pump. *In* The Ca^{2+} Pump of Plasma Membranes. A. F. Rega and P. J. Garrahan, editors. CRC press, Inc., Boca Raton, FL. 137–151.

Glynn, I. M., and J. F. Hoffman. 1971. Nucleotide requirements for sodium-sodium exchange catalyzed by the sodium pump in human red cells. *Journal of Physiology.* 218:239–256.

Grynkiewicz, G., M. Poenie, and R. Y. Tsien. 1985. A new generation of Ca^{2+} indicators with greatly improved fluorescence properties. *Journal of Biological Chemistry.* 260:3440–3450.

Highsmith, S., P. Bloebaum, and K. W. Snowdowne. 1986. Sarcoplasmic reticulum interacts with the Ca^{2+} indicator precursor fura-2-am. *Biochemical and Biophysical Research Communications.* 138:1153–1162.

Jackson, A. P., M. P. Timmermann, C. R. Bagshaw, and C. C. Ashley. 1987. The kinetics of calcium binding to fura-2 and indo-1. *FEBS Letters.* 216:35–39.

James-Kracke, M. R., and J. Chai. 1986. Calmodulin stimulates resting Ca^{2+} transport rate in ghosts containing an ATP regenerating system and quin-2. *Biophysical Journal.* 49:548*a*. (Abstr.)

James-Kracke, M. R., and J. C. Freedman. 1986. Calcium transport monitored by Quin-2 fluorescence in human red blood cells ghosts. *Annals of the New York Academy of Sciences.* 463:389–391.

Klee, C. B., T. H. Crouch, and P. G. Richman. 1980. Calmodulin. *Annual Review of Biochemistry.* 49:489–515.

Knauf, P. A., G. F. Fuhrman, S. Rothstein, and A. Rothstein. 1977. The relationship between anion exchange and net anion flow across the human red blood cell membrane. *Journal of General Physiology.* 69:363–386.

Kotogal, N., R. Colca, and M. L. McDaniel. 1983. Activation of an islet cell plasma membrane (Ca^{2+} + Mg^{2+})-ATPase by calmodulin and Ca-EGTA. *Journal of Biological Chemistry.* 258:4808–4813.

Kratje, R. B., P. J. Garrahan, and A. F. Rega. 1983. The effects of alkali metal ions on active Ca^{2+} transport in reconstituted ghosts from human red cells. *Biochimica et Biophysica Acta.* 731:40–46.

Larsen, F. L., T. R. Hinds, and F. F. Vincenzi. 1978. On the red blood cell Ca^{2+}-pump: an estimate of stoichiometry. *Journal of Membrane Biology.* 41:361–376.

Lew, V. L., S. Muallem, and C. A. Seymour. 1982*a*. Properties of the Ca^{2+}-activated K^+ channel in one-step inside-out vesicles from human red cell membranes. *Nature.* 296:742–744.

Lew, V. L., R. Y. Tsien, C. Miner, and R. M. Bookchin. 1982*b*. Physiological $[Ca^{2+}]_i$ level and pump leak turnover in intact red cells measured using an incorporated Ca chelator. *Nature.* 298:478–481.

Muallem, S., and S. J. D. Karlish. 1979. Is the red cell calcium pump regulated by ATP. *Nature.* 277:238–240.

Muallem, S., and S. J. D. Karlish. 1982. Regulation of the Ca^{2+} pump by calmodulin in intact cells. *Biochimica et Biophysica Acta.* 687:329–332.

Murphy, E., L. Levy, L. R. Berkowitz, E. P. Orringer, S. A. Gabel, and R. E. London. 1986. Nuclear magnetic resonance measurement of cytosolic free calcium levels in human red blood cells. *American Journal of Physiology.* 251:C496–C504.

Niggli, V., E. S. Adunyah, J. T. Penniston, and E. Carafoli. 1981. Purified (Ca^{2+}-Mg^{2+})-ATPase of the erythrocyte membrane: reconstitution and effect of calmodulin and phospholipids. *Journal of Biological Chemistry.* 256:395–401.

Plishker, G. A., P. H. White, and E. D. Cadman. 1986. Involvement of a cytoplasmic protein in calcium-dependent potassium efflux in red blood cells. *American Journal of Physiology.* 251:C535–C540.

Quast, U., A. M. Labhardt, and V. M. Doyle. 1984. Stopped-flow kinetics of the interaction of the fluorescent calcium indicator quin2 with calcium ions. *Biochemical and Biophysical Research Communications.* 123:604–611.

Quist, E. E., and B. D. Roufogalis. 1975. Determination of the stoichiometry of the calcium pump in human erythrocytes using lanthanum as a selective inhibitor. *FEBS Letters.* 50:135–139.

Rasmussen, H. 1989. The cycling of calcium as an intracellular messenger. *Scientific American.* 261:66–73.

Rega, A. F. 1986*a*. Transport of Ca^{2+} and ATP hydrolysis by the Ca^{2+} pump. *In* The Ca^{2+} Pump of Plasma Membranes. A. F. Rega and P. J. Garrahan, editors. CRC Press, Inc., Boca Raton, FL. 67–90.

Rega, A. F. 1986*b*. Other properties and coupling of Ca^{2+} transport and ATP hydrolysis. *In* The Ca^{2+} Pump of Plasma Membranes. A. F. Rega and P. J. Garrahan, editors. CRC Press, Inc., Boca Raton, FL. 91–104.

Richards, D. E., and D. A. Eisner. 1982. Preparation and use of resealed red cell ghosts. *In* Red Cell Membranes: A Methodological Approach. J. C. Ellory and J. D. Young, editors. Academic Press Ltd., London. 165–177.

Rossi, J. P. F. C., P. J. Garrahan, and A. F. Rega. 1981. Vanadate inhibition of active Ca^{2+} transport across human red cell membranes. *Biochimica et Biophysica Acta.* 648:145–150.

Roufogalis, B. D. 1979. Regulation of calcium translocation across the red blood cell membrane. *Canadian Journal of Physiology and Pharmacology.* 57:1331–1349.

Sarkadi, B., A. Enyedi, and G. Gardos. 1987. Conformational changes of the in situ red cell membrane calcium pump affect its proteolysis. *Biochimica et Biophysica Acta.* 899:129–133.

Sarkadi, B., A. Schubert, and G. Gardos. 1979. Effects of calcium-EGTA buffers on active calcium transport in inside-out red cell membrane vesicles. *Experientia.* 35:1045–1047.

Scanlon, M., D. A. Williams, and F. S. Fay. 1987. A Ca^{2+}-insensitive form of fura-2 associated with polymorphonuclear leukocytes: assessment and accurate Ca^{2+} measurement. *Journal of Biological Chemistry.* 262:6308–6312.

Scharff, O., and B. Foder. 1982. Rate constants for calmodulin binding to Ca^{2+}-ATPase in erythrocyte membranes. *Biochimica et Biophysica Acta.* 691:133–143.

Scharff, O., B. Foder, and U. Skibsted. 1983. Hysteretic activation of the Ca^{2+} pump revealed by calcium transients in human red cells. *Biochimica et Biophysica Acta.* 730:295–305.

Schatzmann, H. J. 1973. Dependence on calcium concentration and stoichiometry of the calcium pump in human red cells. *Journal of Physiology.* 235:551–569.

Schatzmann, H. J. 1975. Active calcium transport and Ca^{2+}-activated ATPase in human red cells. *Current Topics in Membranes and Transport.* 5:125–168.

Taverna, R. D., and D. J. Hanahan. 1980. Modulation of human erythrocyte Ca^{2+}/Mg^{2+} ATPase activity by phospholipase A_2 and proteases: a comparison with calmodulin. *Biochemical and Biophysical Research Communications.* 94:652–659.

Tiffert, T., J. Garcia-Sancho, and V. L. Lew. 1984. Irreversible ATP depletion caused by low concentrations of formaldehyde and of calcium-chelator esters in intact human red cells. *Biochimica et Biophysica Acta.* 773:143–156.

Tsien, R. Y., T. Possan, and T. J. Rink. 1982. Calcium homeostasis in intact lymphocytes; cytoplasmic free calcium monitored with a new intracellularly trapped fluorescent indicator. *Journal of Cell Biology.* 94:325–334.

Uto, A., H. Arai, and Y. Ogawa. 1991. Reassessment of fura-2 and the ratio method for determination of intracellular Ca^{2+} concentrations. *Cell Calcium.* 12:29–37.

Varecka, L., and E. Carafoli. 1982. Vanadate-induced movements of Ca^{2+} and K^+ in human red blood cells. *Journal of Biological Chemistry.* 257:7414–7421.

Villalobo, A., L. Brown, and B. D. Roufogalis. 1986. Kinetic properties of the purified Ca^{2+}-translocating ATPase from human erythrocyte plasma membranes. *Biochimica et Biophysica Acta.* 854:9–20.

Vincenzi, F. F., T. R. Hinds, and B. U. Raess. 1980. Calmodulin and the plasma membrane calcium pump. *Annals of the New York Academy of Sciences.* 356:232–244.

Yang, Y.-C., and D. R. Yingst. 1989. Effects of intracellular free Ca and rate of Ca influx on the Ca pump. *American Journal of Physiology.* 256:C1138–C1144.

Yingst, D. R., and J. F. Hoffman. 1978. Changes of intracellular Ca^{2+} as measured by arsenazo III in relation to the K permeability of human erythrocyte ghosts. *Biophysical Journal.* 23:463–471.